Weak Intermolecular Interactions during the Melt Crystallization of Poly(L-lactide) Investigated by Two-Dimensional Infrared Correlation Spectroscopy

Jianming Zhang,[†] Hideto Tsuji,[‡] Isao Noda,[§] and Yukihiro Ozaki*,[†]

Department of Chemistry, School of Science and Technology, Kwansei-Gakuin University, Gakuen, Sanda 669-1337, Japan, Department of Ecological Engineering, Faculty of Engineering, Toyohashi University of Technology, Tempaku-cho, Toyohashi, Aichi 441-8580, Japan, and The Procter & Gamble Company, 8611 Beckett Road, West Chester, Ohio 45069

Received: April 19, 2004; In Final Form: May 16, 2004

The isothermal crystallization behavior of poly(L-lactide) (PLLA) at 150 °C from the melt was monitored by infrared (IR) spectroscopy. The two-dimensional (2D) correlation analysis of time-dependent IR spectra collected during the melt crystallization process revealed details about the intermolecular interaction of the CH_3 and C═O groups and the conformational changes in the C−O−C backbone that are not easily detected by conventional one-dimensional spectra. It was found that the intermolecular interaction of the CH_3 group appears during both the induction period and the growth period of PLLA melt crystallization, while the intermolecular coupling of the C═O group can only be observed during the crystallization period. The order formation of C−O−C backbone during the induction period of PLLA melt crystallization can also be clearly observed in the 2D synchronous spectra. These observations not only provide direct evidence that the distorted 10_3 helix conformation of PLLA chain in α crystals is due to the interchain interactions between CH_3 groups, but also show that the weak interchain interactions play an important role in controlling the nucleation and growth of polymer crystallization.

1. Introduction

Among the family of environmentally friendly biodegradable polymers, poly(L-lactide) (PLLA) ($-[CH_2CH(CH_3)COO]_n-$) has been attracting much attention because of many advantages in its intrinsic properties. For example, the polymer is produced from renewable resources such as starch and exhibits biocompatibility and high mechanical performances comparable to those of commercial polymers.[1−5] Usually, the mechanical properties and chemical stability of a crystalline polymer strongly depend on the morphology and crystal structure. Therefore, the morphology and crystal structure of PLLA fibers, films, and single crystals have been extensively investigated by atomic force microscopy, transmission electron microscopy, X-ray scattering, etc. for the past decade.[6−14]

Depending on the preparation conditions, PLLA crystallizes in three modifications (α, β, and γ forms). The most common polymorph, α form, is obtained by crystallization from solutions or melt and has a 10_3 helical chain conformation as determined by De Santis and Kovacs in 1968.[12] The β form is prepared at high draw ratio and high drawing temperature and is known to take a left-handed 3_1 helical conformation,[10,13] whereas a new γ form produced through epitaxial crystallization was recently described by Cartier et al.[9] Although considerable progress has been made in elucidating the crystalline structure of PLLA, controversial data are still found in the literature. Especially, the crystalline structure of the most common α form has yet to be assigned definitively. For example, Hoogsten et al.[8] observed extra 00*l* reflections that suggest some deviation from a "pure" 10_3 helix conformation. They suggested that the chain conformation is certainly distorted periodically from the regular helix owing to the interchain interactions between CH_3 groups. However, subsequently, Kobayashi et al.[7] proposed the pseudo-orthorhombic (triclinic) unit cell for the α form, in which two chains of PLLA with the same direction are arranged at uneven intervals. The packing of PLLA chains did not seem reasonable, and the agreement between the observed and calculated intensties was poor. By potential energy calculations, Tashiro et al.[14] recently suggested that the periodic chain distortion resulted from the impartial stress distribution due to the interchain interactions. To solve the conflict between the X-ray data and structure assignment of PLLA α crystals, researchers have begun to pay more attention to the effects of intermolecular interactions among PLLA chains.

It is well-known that infrared spectroscopy (IR) is sensitive to local molecular environment. Accordingly, it has been widely used to explore variations in the intra- and intermolecular interactions and structural changes of macromolecules during the melting and crystallization process.[15−17] The crystallization processes of many semicrystalline polymers, such as polyethylene (PE),[18] isotactic polypropylene (iPP),[19] and isotactic polystyrene (iPS),[20] have been extensively investigated by IR spectroscopy. Several papers have been published concerning the IR and Raman spectra of PLA, and the effects of the crystallinity on the spectra have also been discussed.[21−23] However, surprisingly little IR study has been reported on the crystallization process of PLLA. Moreover, it is also noted that there is a large body of work detailing the effects of strong intermolecular interactions, mainly the hydrogen bondings, on the crystalline behavior of semicrystalline polymers.[24−26] However, few reports have so far been concerned with the influence

* To whom correspondence should be addressed. Fax: +81-79-565-9077. E-mail: ozaki@ksc.kwansei.ac.jp.
[†] Kwansei-Gakuin University.
[‡] Toyohashi University of Technology.
[§] Procter & Gamble.

10.1021/jp048308q CCC: $27.50
Published on Web 07/03/2004

of weak interchain interactions on the nucleation and growth of polymers.

Generalized two-dimensional (2D) correlation spectroscopy proposed by Noda,[27−29] which is an extension of the original 2D correlation spectroscopy, has become a very powerful and versatile tool for elucidating subtle spectral changes induced by an external perturbation. It emphasizes spectral features not readily observable in conventional one-dimensional (1D) spectra and probes the specific order of certain events taking place under the influence of a controlled physical variable. The usefulness of the 2D correlation approach results primarily from the enhancement of the spectral resolution that has a physical origin. This effect relies on the dissimilarity among the responses of various submolecular groups absorbing at distinct wavenumbers under a given perturbation. A number of applications of 2D correlation spectroscopy have been reported concerning temperature-, concentration-, and time-dependent spectral changes. Generalized 2D correlation spectroscopy has been applied extensively to analyze IR spectra of polymers for three major reasons:

(1) It has powerful deconvolution ability for highly overlapped bands.

(2) It provides information about inter- and intramolecular interactions by correlating absorption band intensities of different functional groups.

(3) The intensity changes of specific sequence occurring during the measurement can be derived from the analysis of the asynchronous spectra.

These features are ideally suited for studies of the crystallization process of polymers.

We are interested in investigating "what happens" during the induction period of polymer crystallization by IR spectroscopy, which is one of the most important research topics in polymer physics. Recently, we investigated successfully the structural changes taking place during the induction period of iPS cold crystallization by use of 2D correlation analysis.[30] The synchronous and asynchronous correlation spectra of iPS during the induction period clearly elucidated the preordering process of iPS conformation, which may support the theoretical prediction by Olmsted et al.[31] The study also demonstrated that generalized 2D IR correlation spectroscopy is a powerful tool for investigating the structural changes during the induction period of polymer crystallization. In the present study, we explore the intermolecular interactions in PLLA before and after the start of the melt crystallization of PLLA at 150 °C by using 2D correlation analysis. It has been found that the close contact of CH_3 groups among different polymer chains emerges prior to the formation of 10_3 helix conformation, but the intermolecular coupling of C═O stretching vibration mode can only be observed during the formation and packing process of 10_3 helix conformation. These observations not only provide direct evidence that the distorted 10_3 helix conformation of PLLA chain in α crystals is due to the interchain interactions between CH_3 groups, but also show that the weak interchain interactions play an important role in controlling the nucleation and growth of polymer crystallization.

2. Experimental Section

2.1. Material and Preparation Procedures. The synthesis and purification of PLLA ($M_w \cong 150\,000$ g mol^{-1}, $M_w/M_n = 1.8$) used in the present study were performed according to procedures reported previously.[32] A PLLA film for the IR measurement was cast on a KBr window from a 1% (w/v) PLLA chloroform solution. After the majority of the solvent had evaporated, the film was placed under vacuum at room temperature for 48 h to completely remove the residue solvent. The thickness of such prepared polymer film is ca. 10 μm.

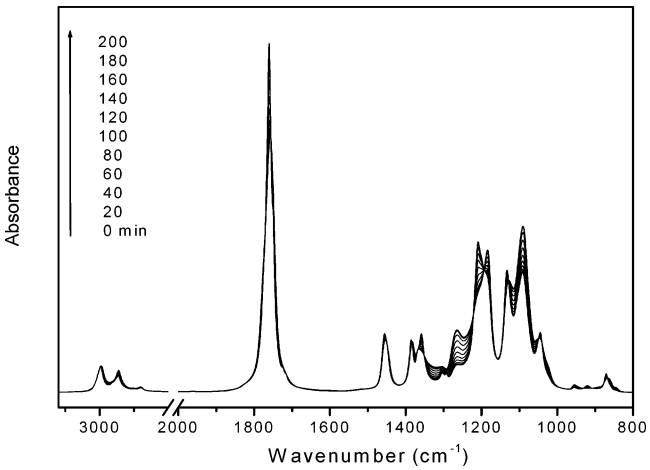

Figure 1. Time-dependent IR spectra in the range of 3200−800 cm^{-1} collected during the melt crystallization of PLLA at 150 °C.

2.2. Fourier Transform IR (FTIR) Spectroscopy. For IR study of the melt crystallization process of PLLA, the sample was set on a homemade variable-temperature cell, which was placed in the sample compartment of a Nicholet Magna 870 spectrometer equipped with an MCT detector. The sample was first heated at 10 °C/min to 200 °C (about 20 °C above the melting point) for 1 min to melt the polymer and completely erase the thermal history. Then, it was cooled at 5 °C/min to 150 °C for isothermal melt crystallization. During the cooling period, we can monitor the structural change of the sample with real-time IR measurement. From the real-time IR spectra, we found that there is no crystallization accruing when sample is cooled to 150 °C and the induction times under such crystallization temperatures are also suitable for our study. IR spectra of the specimen were collected at a 2 cm^{-1} resolution with a 2 min interval during the annealing process. The spectra were obtained by co-adding 16 scans. From IR spectra, it was found that 2 h is enough for finishing the crystallization at 150 °C.

2.3. 2D IR Correlation Analysis. Before the 2D correlation analysis was performed, the IR spectra were preprocessed to minimize the effect of baseline instabilities and other nonselective effects. The frequency regions of interest were truncated first and subjected to a linear baseline correction, followed by offsetting to the zero absorbance value. Ten spectra at an equal temperature interval in a certain wavenumber range were selected for the 2D correlation analysis, which was carried out by use of the software "2D Pocha" composed by D. Adachi (Kwansei-Gakuin University). The temperature-averaged reference spectra are shown at the side and top of the 2D correlation maps for reference. In the 2D correlation maps, regions without dots indicate positive correlation intensities, while those with dots indicate negative correlation intensities.

3. Results and Discussion

First, we investigate IR spectral changes of PLLA in the whole mid-IR region during the crystallization of PLLA. Figure 1 shows the time-dependent IR spectra in the range of 3200−800 cm^{-1} collected during the crystallization of PLLA at 150 °C from melt for 200 min. The enlarged spectra in the 970−850 cm^{-1} region are shown in Figure 2. From Figure 1, it can be seen that three regions of the IR spectra are very sensitive to the structural changes taking place during the melt crystal-

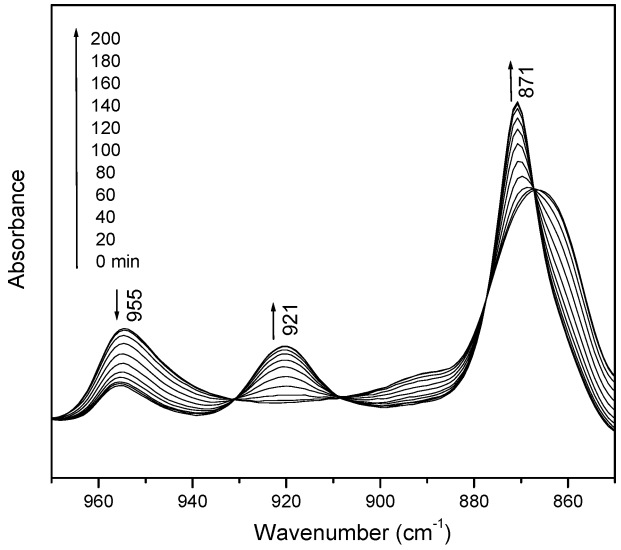

Figure 2. Time-dependent IR spectra in the range of 970−850 cm^{-1} collected during the melt crystallization process of PLLA at 150 °C.

lization of PLLA: the C═O stretching band region of 1860−1660 cm^{-1}, the CH_3, CH bending, and C−O−C stretching band region of 1500−1000 cm^{-1}, and the skeletal stretching and CH_3 rocking band region of 970−850 cm^{-1}. Detailed analysis and discussion on these crystallization-sensitive regions will be described separately below.

3.1. Skeletal Stretching and CH_3 Rocking Region of 970−850 cm^{-1}. It is well-known that PLLA crystallizes into α crystals with the distorted 10_3 helix conformation from solutions or melt. Kister et al.[21] and Cohn and Younes[33] reported that an absorption band at 921 cm^{-1} is characteristic of α crystals. Subsequently, Lee et al.[34] found that this band shows perpendicular dichroism in oriented α films prepared by tensile drawing of an amorphous film at low temperatures. Recently, Kang et al.[23] assigned this band associated with the transition moment perpendicular to the chain axis to the CH_3 rocking mode combined with a minor contribution from the C−COO and O−CH stretching modes of α crystals. The time-dependent spectra in Figure 2 unambiguously reveal that a band at 921 cm^{-1} appears and its intensity increases gradually with the annealing time, which indicates that α crystals are formed during the melt crystallization of PLLA at 150 °C. From refs 21, 23, 33, and 34 we notice that few analyses and assignments have been made for the other two crystallization-sensitive bands at 955 and 871 cm^{-1} in the region of 970−850 cm^{-1}. Obviously, the change of the band at 871 cm^{-1} is similar to that of the band at 921 cm^{-1}, while the intensity of the band at 955 cm^{-1} decreases with the annealing time.

Figure 3 shows the synchronous and asynchronous correlation spectra of PLLA, in the region of 970−850 cm^{-1}, calculated from the spectra in Figure 2. The intensity of a synchronous 2D correlation spectrum $\Phi(\nu_1,\nu_2)$ represents the simultaneous or coincidental changes of spectral intensity variations measured at ν_1 and ν_2; an asynchronous spectrum $\Psi(\nu_1,\nu_2)$, on the other hand, represents sequential or successive changes of spectral intensities measured at ν_1 and ν_2. According to Noda's rule,[28,29] the sign of an asynchronous cross-peak becomes positive, if the intensity change at ν_1 occurs predominantly before ν_2 in the sequential order of *t*. It becomes negative, on the other hand, if the change occurs after ν_2. This rule is, however, reversed if the corresponding synchronous intensity becomes negative; i.e., $\Phi(\nu_1,\nu_2) < 0$. On the basis of this unique feature of asynchronous spectra, we expected to obtain more information about

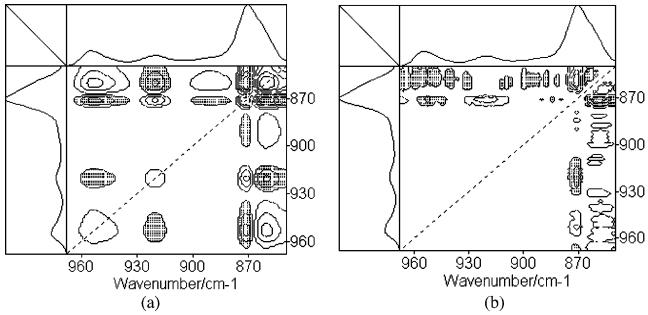

Figure 3. Synchronous (a) and asynchronous (b) 2D IR correlation spectra of PLLA, in the region of 970−850 cm^{-1}, calculated from spectra obtained during annealing at 150 °C.

the origin of the three bands at 955, 921, and 871 cm^{-1}. In the synchronous spectrum shown in Figure 3a, besides the three bands mentioned above, another band located around 860 cm^{-1} can also be deconvoluted effectively. According to the sign of cross-peaks in Figure 3a, the intensities of the bands at 921 and 871 cm^{-1} increase, while those of the bands at 955 and 860 cm^{-1} decrease. When a polymer transitions from the amorphous to the crystalline phase, the intensity of crystalline bands will increase, and the amorphous bands will decrease. Crystalline bands may be caused by the change in the conformation of the chain in the crystal cell of the polymer compared with its conformation in the amorphous state. In the case of the melt crystallization of PLLA, we have already confirmed the formation of α crystals with the 10_3 helix conformation by the band at 921 cm^{-1}. Therefore, it is rational to propose that the 871 cm^{-1} band is also sensitive to the 10_3 helix conformation, and the 955 and 860 cm^{-1} bands are related to the amorphous state of PLLA.

In the asynchronous spectrum (Figure 3b), there are some unexpected and irregular cross-peaks relating to the 860 cm^{-1} band. It has been found that some irregular patterns generated in a 2D asynchronous map may result from small frequency shifts or bandwidth changes.[35,36] Therefore these unexpected and irregular cross-peaks in Figure 3b indicate that the frequency or bandwidth of the band at 860 cm^{-1} changes during the crystallization. This phenomenon also reveals the high sensitivity of an asynchronous 2D correlation spectrum to the fluctuations of experimental spectra.[29,30] Although there is some interference due to the peak shape variation of the band at 860 cm^{-1}, some valuable information still can be obtained from several well-separated cross-peaks. First, according to Noda's rule, from $\Phi(921,871) > 0$, $\Phi(955,871) < 0$ and $\Psi(921,871) > 0$, $\Psi(955,871) < 0$ presented respectively in Figure 3a and Figure 3b, the intensity changes of the 921 and 955 cm^{-1} bands occur prior to that of the 871 cm^{-1} band. Second, of note in Figure 3b is that there is no cross-peak between the bands at 955 and 921 cm^{-1}. This indicates that the changes of these two bands are synchronous. In conclusion, the sequential order for these bands is 955 cm^{-1} ∼ 921 cm^{-1} > 871 cm^{-1}.

In the crystallization process, the intensity of the band at 921 cm^{-1} increases while that of the 955 cm^{-1} band decreases, and their changes are synchronized as shown in the above 2D correlation analysis. The 921 cm^{-1} band is assigned to a 10_3 helix sensitive band, and the band at 955 cm^{-1} is ascribed to an amorphous band. Moreover, these two bands are well separated in the original 1D spectra (Figure 2). Accordingly, it is possible to determine quantitatively the crystallinity of PLLA by use of the two bands. It is interesting to note that both bands at 921 and 871 cm^{-1} are related to the 10_3 helix conformation of PLLA, but their appearance is asynchronous. Kobayashi and

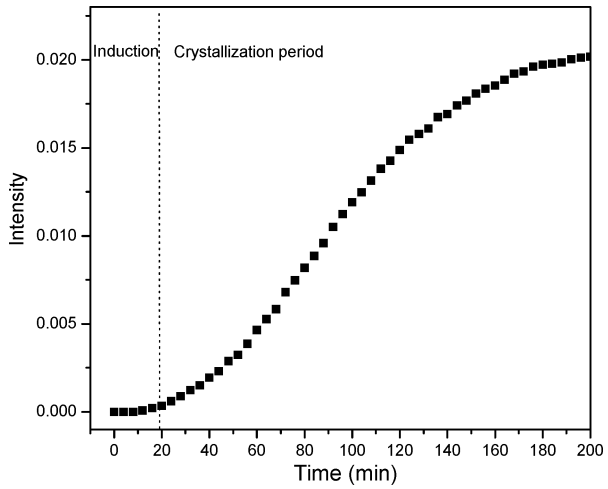

Figure 4. Intensities of the 10_3 conformation sensitive band at 921 cm^{-1} of PLLA as a function of crystallization time at 150 °C.

co-workers[37] introduced the concept of critical sequence length, which depicts the shortest length of the regular sequence with a particular conformation necessary for the appearance of some helix bands. The appearances of the helix bands depend on the sequence length of the helix unit. Therefore, the rational explanation may be that the band at 921 cm^{-1} corresponds to a shorter critical sequence length than that of the band at 871 cm^{-1}.

Usually, the induction period before crystal growth is determined by differential scanning calorimetric (DSC) measurement, and the crystallization kinetics during thermal annealing can be followed by using the FTIR technique. However, the induction periods studied by these two methods are obviously different. The reason is that the DSC technique measures the heat flow during the crystallization of polymer crystals, while IR spectroscopy is sensitive to local molecular environment. In other words, DSC responds to three-dimensional order of the crystalline structure, whereas the FTIR technique measures the short-range order that depends on the degree to which the vibrational mode is coupled to adjacent vibrations. The short-range order can exist without the presence of long-range order. Thus, it is reasonable to predict that the induction time measured by DSC is longer than that measured by IR spectroscopy. To elucidate the inter- or intramolecular interactions before and after the formation of short-range ordered structure, we characterize crystallization kinetics of PLLA during the melt crystallization by monitoring the peak intensity of the helix conformation sensitive band as a function of annealing time. Figure 4 plots the intensity of the band at 921 cm^{-1} as a function of crystallization time at 150 °C. It can be seen from the plot that the induction time is about 20 min for the melt crystallization of PLLA at 150 °C.

3.2. C═O Stretching Region and the CH_3, CH Bending, and C−O−C Stretching Regions. The evolution of spectra in the regions of 1500−1000 and 1860−1660 cm^{-1} during the cold crystallization are shown in parts a and b, respectively, of Figure 5. Difference spectra obtained by the subtraction of the initial spectrum from the spectra in Figure 5a,b are also displayed in Figure 5c,d. It is noted in the difference spectra that band splittings are clearly observed in both regions. In the range of 1500−1300 cm^{-1}, a band at 1454 cm^{-1} assigned to the CH_3 asymmetric deformation mode turns into two bands at 1457 and 1442 cm^{-1} during the crystallization. In the C═O stretching region, two split bands appear at 1753 and 1745 cm^{-1} with the evolution of the crystallization.

Usually, the fundamental modes of a single polymer chain are split into various spectral components in the crystal if the intermolecular forces between polymer chains are sufficient.[38] Physically, such splitting, called correlation field splitting or factor group splitting, occurs as a result of the resonance interactions of analogous vibrations undergone by individual chains in the unit cell. The number of theoretically expected bands depends on the number of molecules in the unit cell. Polyethylene, which has closer chains than any other polymer, is a typical example of exhibiting the largest crystal field splitting. Since the splitting is very sensitive to the separation of polymer chains, very few polymers exhibit the crystal field splitting observed in specific cases. However, even if most polymers do not exhibit crystal field splitting due to intermolecular or crystalline packing, band pairs can arise from intramolecular helical splitting, such as in the case of polypropylene. That is, polymers not only exhibit resonance splitting of bands associated with interaction between analogous groups along the polymer chain but also show splitting of certain vibrations related to intramolecular interaction because of the helical chain structure.

According to the crystal structure of PLLA revealed by X-ray crystallography,[8] the PLLA chains form a distorted 10_3 helical structure in α crystals, and its crystal unit cell contains two left-handed helical molecules in antiparallel orientation. The distance between the neighboring C═O groups along the chain can be estimated to be 3.26 Å from the crystal structure revealed by X-ray crystallography, which is larger than the distance (∼2.7 Å) for inducing the dipole−dipole interaction.[39] Therefore, it seems very likely that the splitting of C═O stretching band comes from the interchain interaction and not from the intrachain interaction during the crystallization of PLLA. Since the CH_3 groups are separated alternately by the C═O groups along the polymer chain, and the transition moment of $\delta_{as}(CH_3)$ is parallel to the chain axis of PLLA, the splitting of CH_3 asymmetric deformation mode may also be caused by the dipole−dipole interaction due to the interchain packing of the CH_3 groups in the crystal unit cell of PLLA.

To investigate how interchain interactions influence nucleation and growth of PLLA during the isothermal crystallization from melt, we further investigate the 2D correlation spectra of PLLA calculated from the spectra obtained in the induction period and growth period, respectively. The synchronous 2D spectrum $\Phi(\nu_1,\nu_2)$ in the range of 1500−1340 cm^{-1} generated from the time-dependent spectra collected in the induction period (from 0 to 18 min) is displayed in Figure 6a. For comparison, the corresponding synchronous spectrum calculated from the data recorded after the induction period (from 20 to 200 min) is given in Figure 6b. In both 2D spectra, it can be seen that highly overlapped peaks in the 1500−1340 cm^{-1} region are deconvoluted effectively by spreading the peaks along the second spectral dimension. Surprisingly, Figure 6a and Figure 6b are very similar. The splitting of $\delta_{as}(CH_3)$ can be clearly observed in both the induction period and the growth period, which indicates that the CH_3 groups among different PLLA chains are already in close contact prior to the crystal growth in PLLA. On the basis of the results of X-ray crystallography, some researchers have suggested that the interchain contacts between CH_3 groups force this distortion of chain conformation in α crystals of PLLA, in a way similar to the helix conformation of poly(l-alanine), which is the polypeptide analogous of poly(L-lactide).[40] Our 2D IR spectra show that the formation of the initial helix chain conformation is also interfered with by the weak interchain interactions between CH_3 groups.

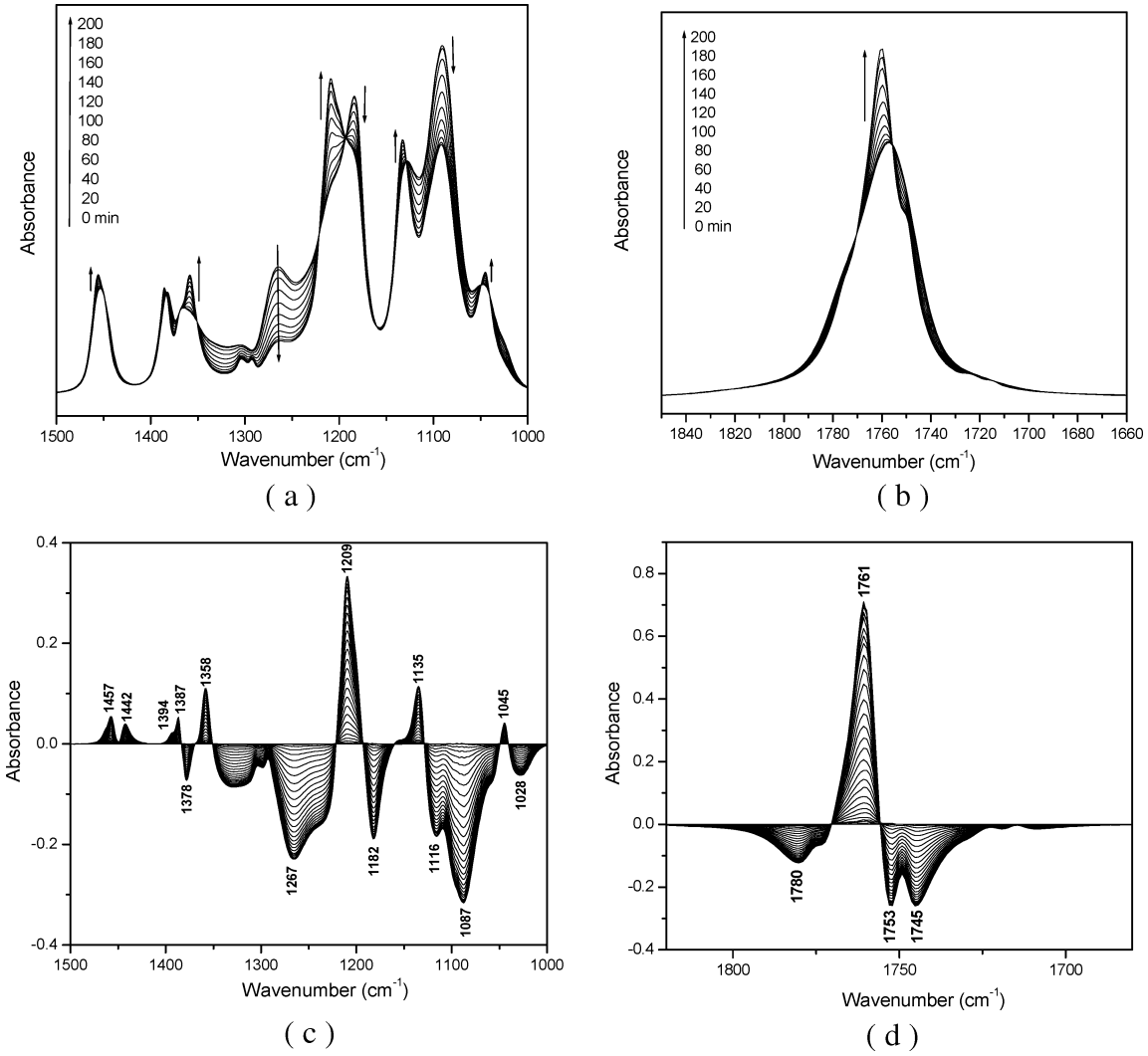

Figure 5. (a) Temporal changes of the IR spectrum in the regions of (a) 1500−1000 and (b) 1860−1600 cm^{-1} during melt crystallization of PLLA at 150 °C. The spectra displayed are those measured with a 20 min interval. (c) and (d) Difference spectra calculated by subtracting the initial spectrum from the spectra shown in (a) and (b), respectively.

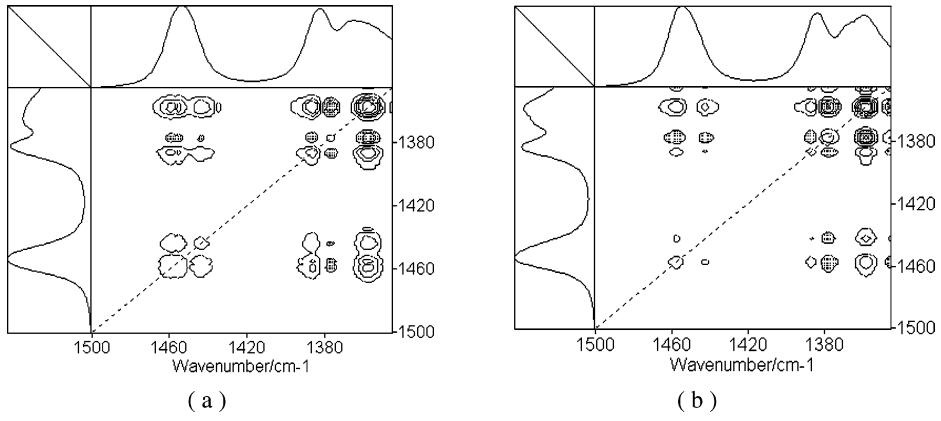

Figure 6. Synchronous correlation spectra of PLLA, in the region of 1500−1300 cm^{-1}, calculated from spectra obtained during melt crystallization at 150 °C. (a) Spectra obtained from 0 to 18 min; (b) those from 20 to 200 min.

Parts a and b, respectively, of Figure 7 show the synchronous 2D spectra in the C═O stretching vibration region generated from the time-dependent spectra collected in the induction period (from 0 to 18 min) and the growth period (from 20 to 200 min) during the melt crystallization of PLLA at 150 °C. In Figure 7a, only one cross-peak develops in the region of 1760−1730 cm^{-1}, while two obvious cross-peaks which reflect the splitting of the C═O stretching vibration mode can easily be found in Figure 7b. This indicates that the C═O groups among different PLLA chains do not form close contact at the early stage of PLLA crystallization.

The synchronous 2D spectra in the region of 1300−1000 cm^{-1}, which is mainly related to the C−O−C stretching vibrations, are displayed in Figure 8. Figure 8a shows the synchronous 2D spectrum generated from the time-dependent spectra collected in the induction period (from 0 to 18 min),

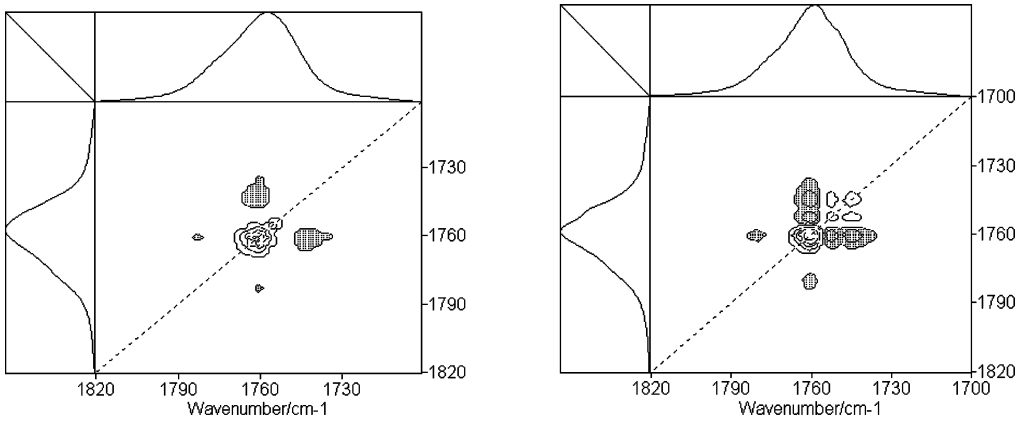

Figure 7. Synchronous correlation spectra of PLLA, in the region of 1820−1700 cm^{-1}, calculated from spectra obtained during melt crystallization at 150 °C. (a) Spectra obtained from 0 to 18 min; (b) those from 20 to 200 min.

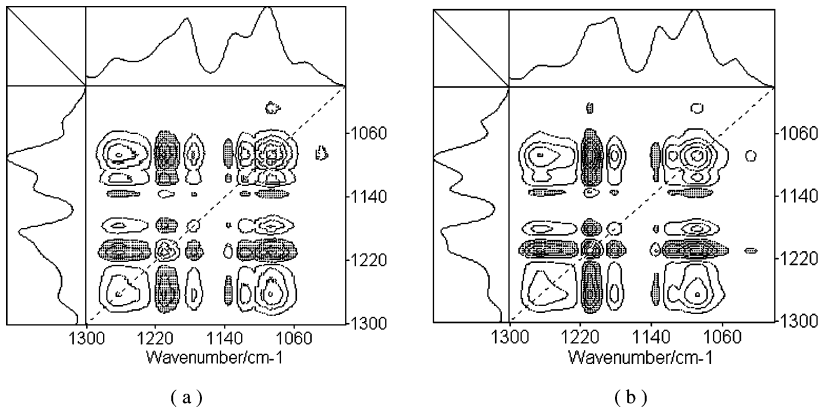

Figure 8. Synchronous correlation spectra of PLLA, in the region of 1300−1000 cm^{-1}, calculated from spectra obtained during melt crystallization at 150 °C. (a) Spectra obtained from 0 to 18 min; (b) those from 20 to 200 min.

while Figure 8b shows the synchronous 2D spectrum in the growth period (from 20 to 200 min). In the original IR spectra shown in Figure 5a and the corresponding difference spectra shown in Figure 5c, one can easily see that obviously spectral changes appear in the range of 1300−1000 cm^{-1} with the evolution of PLLA crystallization. Therefore, these spectral changes should reflect the structural order of the C−O−C backbone. From Figure 8, it can be seen that the 2D synchronous spectra generated from the data collected from the introduction period and growth period are very similar to each other, indicating that the order formation of C−O−C backbone already emerges in the induction period of PLLA crystallization.

4. Conclusion

In the present study, we have investigated the isothermal crystallization behavior of PLLA at 150 °C from melt by FTIR spectroscopy. To elucidate the intermolecular interaction before and after the formation of short-range-ordered structure, the skeletal stretching and CH_3 rocking bands in the 1000−800 cm^{-1} region were investigated by 2D IR correlation analysis. It has been found that both the bands at 921 and 871 cm^{-1} are related to the 10_3 helix conformation of PLLA, and that the band at 921 cm^{-1} corresponds to a shorter critical sequence length than that of the band at 871 cm^{-1}. It has also been revealed that the bands at 955 and 860 cm^{-1} reflect the amorphous state of PLLA. In the present study, the induction period is derived from the crystallization kinetic curve of PLLA melt crystallization characterized by plotting the peak intensity of the helix conformation sensitive 921 cm^{-1} band as a function of annealing time.

During the melt crystallization of PLLA, the band splittings of CH_3 asymmetric deformation mode and C═O stretching mode can be clearly observed in the time-dependent IR spectra. Considering the crystal structure revealed by X-ray crystallography, the origins of the two band splittings have been assigned to the interchain interaction. From the 2D correlation analysis, it has been found that the CH_3 groups form close interchain contact during the induction period. In other words, the formation of the initial helix chain conformation is already interfered with by the weak interchain interactions between the CH_3 groups. On the other hand, the C═O groups among different PLLA chains do not form close contact at the early stage of PLLA crystallization. These observations have also provided direct evidence that the distorted 10_3 helix conformation of PLLA chain in α crystals is due to the interchain interactions between bhe CH_3 groups. Moreover, the order formation of C−O−C backbone during the induction period of PLLA crystallization can also be clearly observed in the 2D synchronous spectra.

Acknowledgment. Jianming Zhang thanks the Japan Society for the Promotion of Science (JSPS) for financial support.

References and Notes

(1) Ikada, Y.; Tsuji, H. *Macromol. Rapid Commun.* **2000**, *21*, 117.
(2) Tsuji, H.; Ikada, Y. *J. Appl. Polym. Sci.* **1998**, *67*, 405.

(3) Tsuji, H.; Ikada, Y. *Macromol. Chem. Phys.* **1996**, *197*, 3483.
(4) Urayama, H.; Kanamori, T.; Kimura, Y. *Macromol. Mater. Eng.* **2002**, *287*, 116.
(5) Dorgan, J. R. *Poly(lactic acid) Properties and Prospects of an Environmentally Benign Plastic*; American Chemical Society: Washington, DC, 1999; pp 145−149.
(6) Eling, B.; Gogolewski, S.; Pennings, A. J. *Polymer* **1982**, *23*, 1587.
(7) Kobayashi, J.; Asahi, T.; Ichiki, M.; Okikawa, A.; Suzuki, H.; Watanabe, T.; Fukada, E.; Shikinami, Y. *J. Appl. Phys.* **1995**, *77*, 2957.
(8) Hoogsteen, W.; Postema, A. R.; Pennings, A. J.; ten Brinke, G. *Macromolecules* **1990**, *23*, 634.
(9) Cartier, L.; Okihara, T.; Ikada, Y.; Tsuji, H.; Puiggali, J.; Lotz, B. *Polymer* **2000**, *41*, 8909.
(10) Puiggali, J.; Ikada, Y.; Tsuji, H.; Cartier, L.; Okinara, T.; Lotz, B. *Polymer* **2000**, *41*, 8921.
(11) Brizzolara, D.; Cantow, H.-J.; Diederichs, K.; Keller, E.; Domv, A. J. *Macromolecules* **1996**, *29*, 191.
(12) De Santis, P.; Kovacs, J. *Biopolymers* **1968**, *6*, 299.
(13) Kalb, B.; Pennings, A. J. *Polymer* **1980**, *21*, 607.
(14) Tashiro, K.; Sasaki, S.; Kobayashi, M. *Macromolecules* **1996**, *29*, 7460.
(15) Chalmers, J. M.; Hannah, R. W.; Mayo, D. W. Spectra-structure correlations: Polymer spectra. In *Handbook of Vibrational Spectroscopy*; Chalmers, J. M., Griffiths, P. R., Eds.; John Wiley & Sons: Chichester, UK, 2002; Vol. 4, pp 1893−1918.
(16) Koenig, J. L. *Spectroscopy of Polymers*; American Chemical Society: Washington, DC, 1992.
(17) Mallapragada, S. K.; Narasimhan, B. Infrared Spectroscopy in Analysis of Polymer Crystallinity. In *Encyclopedia of Analytical Chemistry*; Meyers, R. A., Ed.; John Wiley & Sons: Chichester, UK, 2000; pp 7644−7658
(18) Bulkin, B. J.; Lewin, M.; DeBlase, F. J. *Macromolecules* **1985**, *29*, 2587.
(19) Zhu, X. Y.; Yan, D. Y.; Fang, Y. P. *J. Phys. Chem. B* **2001**, *105*, 12461.
(20) Duan, Y. X.; Zhang, J. M.; Shen, D. Y.; Yan, S. K. *Macromolecules* **2003**, *36*, 4847.
(21) Kister, G.; Cassanas, G.; Vert, M. *Polymer* **1998**, *39*, 267.
(22) Qin, D. R.; Kean, R. T. *Appl. Spectrosc.* **1998**, *52*, 488.
(23) Kang, S.; Hsu, S. L.; Stidham, H. D.; Smith, P. B.; Leugers, M. A.; Yang, X. *Macromolecules* **2001**, *34*, 4542.
(24) Jiang, H. J.; Wu, P. Y.; Yang, Y. L. *Biomacromolecules* **2003**, *4*, 1343.
(25) Skrovanek, D. J.; Painter, P. C.; Coleman, M. M. *Macromolecules* **1986**, *19*, 699.
(26) Heintz, A. M.; McKiernan, R. L.; Gido, S. P.; Penelle, J.; Hsu, S. L.; Sasaki, S.; Takahara, A.; Kajiyama, T. *Macromolecules* **2002**, *35*, 3117.
(27) Noda, I. *Appl. Spectrosc.* **1993**, *47*, 1329.
(28) Noda, I. *Appl. Spectrosc.* **2000**, *54*, 994.
(29) Noda, I.; Dowrey, A. E.; Marcott, C.; Story, G. M.; Ozaki, Y. *Appl. Spectrosc.* **2000**, *54*, 236.
(30) Zhang, J. M.; Duan, Y. X.; Shen, D. Y.; Yan, S. K.; Noda, I.; Ozaki, Y. *Macromolecules* **2004**, in press.
(31) Olmsted, P. D.; Poon, W. C. K.; McLeish, T. C. B.; Terrill, N. J.; Ryan, A. J. *Phys. Rev. Lett.* **1998**, *81*, 373.
(32) Tsuji, H.; Ikada, Y. *Polymer* **1999**, *40*, 6699.
(33) Cohn, D.; Younes, H. *J. Biomed. Mater. Res.* **1988**, *22*, 993.
(34) Lee, J. K.; Lee, K. H.; Jin, B. S. *Eur. Polym. J.* **2001**, *37*, 907.
(35) Czarnecki, M. A. *Appl. Spectrosc.* **2000**, *52*, 1583.
(36) Huang, H.; Malkov, S.; Coleman, M.; Painter, P. *Macromolecules* **2003**, *36*, 8148.
(37) Kobayashi, M.; Nakaoki, T.; Ishihara, N. *Macromolecules* **1990**, *23*, 78.
(38) Nikimin, V. N.; Volchek, B. Z. *Russ. Chem. Rev.* **1968**, *37*, 225.
(39) Lagaron, J. M. *Macromol. Symp.* **2002**, *184*, 19.
(40) Fraser, R. D. B.; MacRae, T. P. *Conformation in Fibrous Proteins*; Academic Press: New York, 1973.